Multi-transceiver simulation modules for free-space optical mobile ad hoc networks

Mehmet Bilgi and Murat Yuksel

University of Nevada - Reno, CSE Department,
MS 171 1664 N. Virginia Street, Reno, NV 89557, USA.

ABSTRACT

This paper presents realistic simulation modules to assess characteristics of multi-transceiver free-space-optical (FSO) mobile ad-hoc networks. We start with a physical propagation model for FSO communications in the context of mobile ad-hoc networks (MANETs). We specifically focus on the drop in power of the light beam and probability of error in the decoded signal due to a number of parameters (such as separation between transmitter and receiver and visibility in the propagation medium), comparing our results with well-known theoretical models. Then, we provide details on simulating multi-transceiver mobile wireless nodes in Network Simulator 2 (NS-2), realistic obstacles in the medium and communication between directional optical transceivers. We introduce new structures in the networking protocol stack at lower layers to deliver such functionality. At the end, we provide our findings resulted from detailed modeling and simulation of FSO-MANETs regarding effects of such directionality on higher layers in the networking stack.

Keywords: Free-space-optics, wireless simulation, FSO propagation

1. INTRODUCTION AND MOTIVATION

Wireless communication has traditionally been realized via omnidirectional radio frequency. Radio frequency has the major advantage of propagating in all directions enabling a receiver to roam inside the transmission sphere without experiencing a link disruption, although, it may encounter fading and hidden nodes as obstacles hurting the uniformity of the signal and new communicating nodes present in the propagation medium. Nevertheless, a typical RF-enabled node will have a large throughput gap with optical backbone of the network which reveals the last mile problem.[1–3] Pushing more aggressive medium access control (MAC) protocols that operate in much finer grained time scales and employing innovative multihop hierarchical cooperative MIMO[4] techniques remedy the issue partially in the cost of increased complexity. Marginal benefit of such approaches have become smaller due to the increased saturation of the RF spectrum. The throughput gap between optical backbone and the wireless last-mile calls for more radical approaches involving wireless spectrum bands physically much larger than the RF.

Free-space-optical (FSO) (i.e., optical wireless) communication provides an attractive approach complementary to the legacy RF-based wireless communication. Most significant difference between FSO and RF is the requirement of line-of-sight in FSO, adding *space-division multiplexing* (i.e., spatial reuse) to already known multiplexing techniques such as wave-length and time division multiplexing. RF suffers from increased power consumption per interface compared to FSO because of the significantly larger volume of medium that needs to be covered by an individual interface. RF-based communication also has a greater need to employ complex security protocols to address security concerns that rise because of the higher risk of interception especially in military applications.

A typical FSO transmitter (e.g., LASER, VCSEL or LED) forms a cone shaped volume in 3 dimensions (Figure 1) in which a potential receiver equipped with a photo detector can receive the signal. The exact shape of this cone is determined by the transmission power (for range) and divergence angle. A LASER has the smallest (in micro radian range) and an LED has the widest (a few hundred milli radians) divergence angle of the three types of transmitters. FSO can operate in large swathes of unlicensed spectrum reaching speeds up to $\sim$1 Gbps. Additionally, FSO transceivers have much smaller

---

Further author information: (Send correspondence to M. Bilgi)
Mehmet Bilgi: E-mail: mbilgi@cse.unr.edu,
Murat Yuksel: E-mail: yuksem@cse.unr.edu
Phone: +1 (775) 327 2246, Fax: +1 (775) 784 1877

form factors, are less power-consuming (100 microwatts for 10-100 Mbps), very reliable (lifetime of more than 10 years), cheap and offer highly directional beams for spatial reuse and security.

Simulation efforts of free-space-optical communication have primarily focused on physical propagation models.[5,6] Researchers also worked on numerical analysis of the wireless optical communication and especially considered error analysis of the channel in extreme scenarios such as atmospheric turbulence.[7–9] Our focus is mainly on simulating *multi-transceiver FSO structures* with an attention to line-of-sight requirement, 3-D realistic obstacles, obstacle avoiding mobility generation and necessary mechanisms in the networking stack to accomplish such goals.

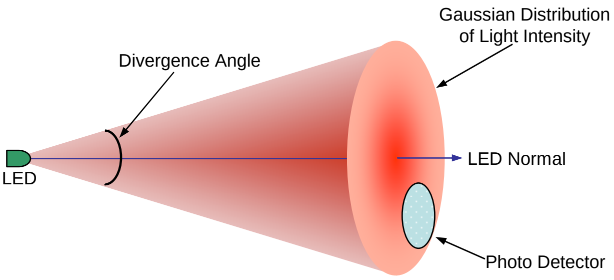

Figure 1. Gaussian distribution of light intensity at the receiver plane.

Network Simulator 2[10] is a widely-used open source discrete event simulation platform for networking research. NS-2 has been developed and maintained by the research community since 1989, letting contributors to enhance its capabilities by implementing various protocols and communication models. Hence, the platform allowed researchers to observe many important phenomenons in wireless networking. Physical free-space-optical propagation model along with directional communication did not exist in NS-2 prior to our contribution. Our contribution will enable researchers to investigate the challenges and merits of multi-element networking nodes with optical transceivers. Our effort is on accurately simulating propagation model[11] of FSO communication, line-of-sight (LOS) requirement for two communicating antennas, the drop in the received power with respect to separation between antennas, and error behavior. Our study considers visibility in the medium, divergence angles of transmitters, field of view of photo-detectors, and surface areas of transceiver devices to identify their effect on the communication performance.

We present a transceiver structure (consisting of an LED and a photo-diode) that has a divergence angle which also determines the field of view of the transceiver. The divergence angle of a transceiver is very fundamental to our contribution since it is the main factor that determines if two transceivers are aligned with each other. Prior to our work, a wireless (RF) link in a packet-based simulator has traditionally been implemented in an omnidirectional way; hence, there was not a way to establish directions links that can use the same frequency band simultaneously without interfering one another. We implemented NS-2 enhancement modules that can:

- Create spherical, circular and tabular FSO nodes with multiple directional interfaces on them,
- Determine the existence of directional links between transceivers of different nodes and deliver packets accordingly,
- Mimic the characteristics of an FSO link in power reception, noise, bit error rate profiles,
- Acknowledge the existence of 3-D obstacles that can disturb directional links,
- Generate mobility scenarios (based on random waypoint) for wireless nodes enabling them to avoid obstacles,
- Let physical layer to gather localization information and present abstracted information to upper layers for further processing.

The rest of the paper is organized as follows: In Section 2, we present the well-known theoretical model for FSO propagation in a non-turbulent medium. We give the details of our NS-2 implementation in Section 3. Section 4 provides the results of our experiments to show the power and theoretical error probability behavior from our FSO simulation modules. Lastly, we summarize our work in Section 5.

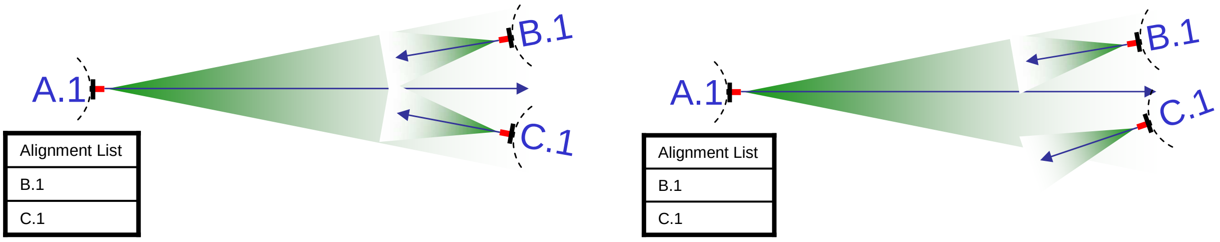

(a) A.1 has bi-directional alignment with both B.1 and C.1
(b) A.1 has only uni-directional alignment with C.1

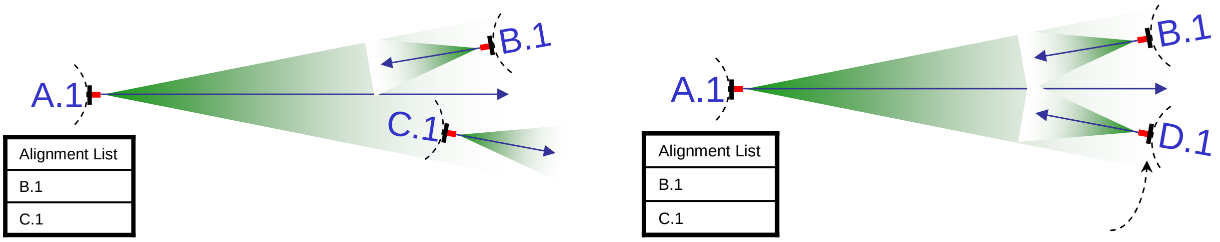

(c) A.1 has lost alignment with C.1
(d) D.1 gets in the LOS of A.1

Figure 2. Types of possible alignment loss/gain during a timer period.

2. THEORETICAL FSO PROPAGATION MODEL

We used well-known FSO propagation models[11] to simulate power attenuation characteristics of an FSO signal. LEDs' light intensity profile follows the Lambertian law,[11] i.e., intensity is directly proportional to the cosine of the angle from which it is viewed. At a distance Z, let the received power along the beam be P_Z. Based on the Lambertian law, at an arbitrary angle α from the vertical axis and at a distance Z, the intensity would be: $P_{\alpha,Z} = P_Z cos(\alpha)$. For edge-emitting LEDs, this is improved by a factor u in the power of cosine, i.e. the intensity is given by: $P_{\alpha,Z} = P_Z cos^u(\alpha)$.

Also, as a generic definition for all FSO transmitters, the beam radius w_Z at the vertical distance Z is defined as the radial distance at which the received power is $\frac{1}{e^2}P_Z$. So, the divergence angle θ is the special value of α, where the ratio $P_{\alpha,Z}/P_Z = 1/e^2$ holds, which means θ can be calculated by $\theta = tan^{-1}(w_Z/Z)$.

FSO propagation is affected by both the atmospheric attenuation A_L and the geometric spread A_G, which practically necessitates the source power to be greater than the power lost. The *geometric attenuation* A_G is a function of transmitter radius γ, the radius of the receiver (on the other receiving FSO node) ς cm, divergence angle of the transmitter θ and the distance between the transmitting node and receiving node R:

$$A_G = 10\log\left(\frac{\varsigma}{\gamma + 200R\theta}\right)^2$$

The *atmospheric attenuation* A_L consists of absorption and scattering of the laser light photons by the different aerosols and gaseous molecules in the atmosphere. The power loss due to atmospheric propagation is given by Bragg's Law[11] as:

$$A_L = 10\log(e^{-\sigma R})$$

where σ is the attenuation coefficient consisting of atmospheric absorption and scattering. For the wavelengths used for FSO communication, Mie scattering dominates the other losses, and therefore is given by:[12]

$$\sigma = \frac{3.91}{V}\left(\frac{\lambda}{550}\right)^{-q}.$$

In the above formulation of σ, V is the atmospheric visibility in kilometers, q is the size distribution of the scattering particles whose value is dependent on the visibility:

$$q = \begin{cases} 1.6 & V \geq 50\text{km} \\ 1.3 & 6\text{km} \leq V < 50\text{km} \\ 0.583V^{1/3} & V < 6\text{km} \end{cases}$$

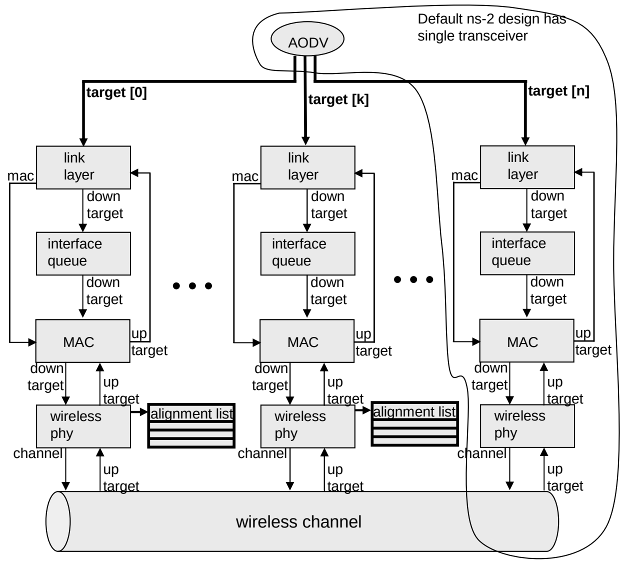

(a) FSO node structure with a separate stack for each optical transceiver. AODV is modified so that it is capable of handling multiple network interfaces. WirelessPhy is also modified to keep a list of aligned transceivers.

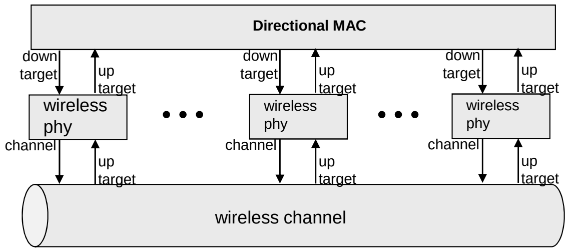

(b) Presenting multiple transceivers as a single network interface to the routing agent using a directional MAC. (Partial representation of node structure.)

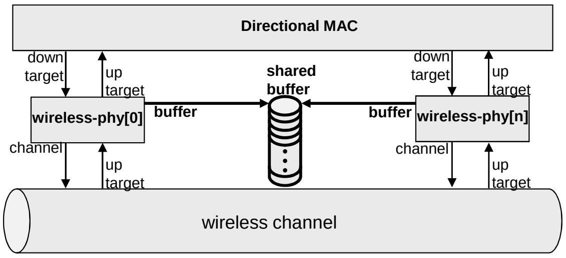

(c) Enabling shared buffering among multiple transceivers in a group or in the node.

Figure 3. Various types of multi-transceiver wireless node designs in NS-2.

3. IMPLEMENTATION IN NETWORK SIMULATOR 2

Our contribution (Figure 3(a)) includes a full implementation of FSO propagation model to calculate source and reception power of packets under relevant parameters such as atmospheric attenuation, visibility, Gaussian-distributed geometric beam spread (Figure 1), photo-detector threshold, transmitter and receiver diameters, divergence angle, desired error probability per bit and noise (Table 4(b)). We use all the above parameters to determine the reception power of a transmission using the theoretical models discussed in Section 2. We also take interference into consideration (Figure 4(a)) while determining signal-to-noise ratio since the interference in FSO is inherently different from RF in the sense that it is directional. We consider all possible directional FSO signals in the medium and determine the level of interference. This is essentially the interference coming from neighboring transceivers, which is conceptually similar to the RF interference.

3.1 Alternative Multi-Element Node Designs

We start with a basic node implementation in NS-2 that satisfies the initial set of requirements for simulating FSO-MANETs. Essentially, our current implementation (Figure 3(a)) is capable of handling multiple transceivers placed on the surface of a node with a spherical, circular or array shape. The Ad-hoc On-Demand Distance Vector (AODV)[13] routing agent is modified to leverage multiple physical links. From the routing agent to channel, we create the chain of internal structures for each transceiver. Furthermore, we introduce alignment lists for each multi-transceiver node to keep track of its aligned target transceivers.

Our current implementation can determine whether given two transceivers are in each others' line of sight in 3 dimensions. While determining the outcome, we take obstacles in the environment into account. We consider FSO nodes with known diameters as obstacles themselves. Our implementation also features simple obstacle representation in 3-D such as buildings. Additionally, we devised an intuitive obstacle avoiding random waypoint mobility scenario generator to be used for each node in city simulations where we have multiple stationary obstacles such as buildings, cars and people.

Alternative to the design depicted in Figure 3(a), we propose a second design that eliminates the awareness of routing agent about multiple transceivers. In this design (Figure 3(b)), we merge interface queues and link layer objects, which reduces the memory footprint of the simulation as well. Additionally, we propose to change the MAC implementation, so that it can handle multiple transceivers and it is aware of the directionality of the underlying physical links. This enables

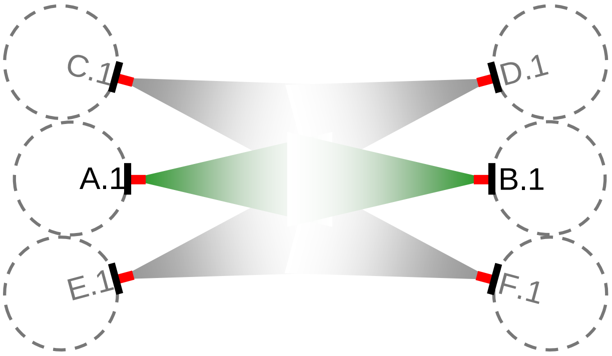

Parameter Name	Default Value
Visibility	6 km
Number of interfaces	8
Transmission range and separation between nodes	30 m
Divergence angle	1 rad
Photo detector diameter	5 cm
LED diameter	0.5 cm
Per-bit error probability	10^{-6}
Noise	1.1428e-12 Watt
Capture threshold	1.559e-11 Watt
Receive threshold	3.652e-10 Watt

(a) Noise in FSO transmission: transceivers C.1, D.1, E.1 and F.1 contribute to the noise for the communication between A.1 and B.1.

(b) Table of default values common to each simulation set in our experiments.

Figure 4. Optical noise and default parameter table.

MAC to make simultaneous transmissions and receptions through different transceivers unlike an ordinary 802.11 MAC. We shall still keep alignment lists for each transceiver, although they are not shown in the figure.

We propose a third design in Figure 3(c). This design introduces a shared buffer among transceivers. We create a fixed-sized FIFO buffer that holds packets which `wireless-phy` (interface) object receives from queue and this interface is no longer is aligned to. Hence, whenever the interface is idle, MAC can schedule transmission of such packets through the correct interface. Such a secondary buffering mechanism is especially helpful in the case of mobility.

3.2 Directional Optical Link Implementation

The directional FSO antenna model that we used has 3-D pointing and divergence angle features as well as diameters of LED/transmitter and photo-detector components. The light beam forms a cone shape in 3-D (Figure 1) as it propagates away from the source. Divergence angle of the transmitting LED dictates the shape of propagation. We use a Gaussian distribution of light intensity when considering a cross cut of this cone. On the receiving side, the photo detector also has a field of view which is assumed to be the same with LED's in the transceivers we simulate.

At a given time, the transceivers in the system form such directional optical links. Those links stay unchanged as long as there is no mobility of either end. With mobility involved, each transceiver can be aligned or can get misaligned to a number of other transceivers. To keep track of such alignment and misalignment events, we implemented a timer mechanism for periodic checking and establishment of LOS alignment lists for each transceiver. We use a new alignment-table-based channel model for delivering packets only to the candidate receiver antennas that reside in the transmitter's alignment list.

Whenever the channel chooses to deliver a packet to a receiver, we take the transmission power and spread it in a Gaussian manner onto a circular area which makes the cross-cut of the illumination cone (Figure 1). Then, we calculate the amount of light that drops on the surface of the receiver using its diameter, its separation from the transmission normal and the angle it makes with the transmission normal. If the received power is greater than carrier sense threshold, then the packet is considered for noise for the currently received packet, if there is any. If the power is greater than receive threshold, then it is considered for reception. After deciding the received power level, we need to determine if the packet is erroneous. We take the reception power of the packet and calculate the theoretical bit error probability using the visibility in the medium, distance between transmitter and receiver and noise. From this bit error probability we calculate the probability that the whole packet can be received without any bit errors. Lastly, drawing from a uniform random variable decides if this packet should be captured without any errors or contribute to the interference.

3.3 Alignment Lists and Alignment Timer

We implemented a timer mechanism in NS-2 that goes off every half-a-second (which can be tuned) and determines the alignments among the transceivers. This timer mechanism corresponds to "automatically" re-checking availability of

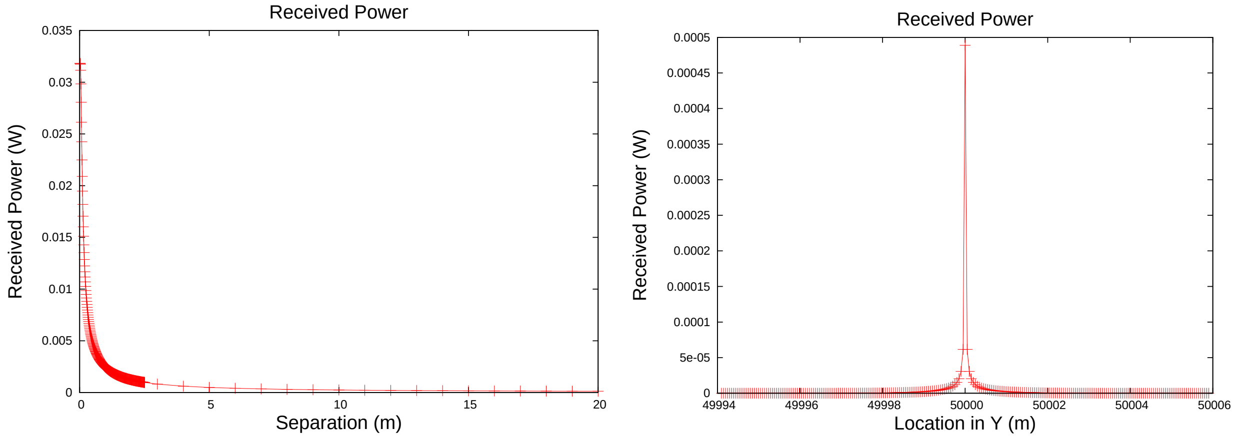

(a) Received power drops significantly as the receiver is moved away from the transmitter. Transmit power is calculated for 10 m range, 6 km visibility, 5 cm receiver diameter, 0.5 cm transmitter diameter and 1 rad divergence angle.

(b) Received power drops significantly as the receiver is moved away from the normal of the transmitter. Samples are taken with 5 m separation from transmitter.

Figure 5. Received power versus separation in both X and Y axis.

LOS alignment. An ongoing transmission may experience a disconnection due to mobility, sway or vibration of either nodes.[14–16] In such a disconnection, automatic alignment checking can be considered as the “search” phase before starting to send data. The search phase discovers possible alignment establishments which are discovered via the alignment timers in our simulations. In simulation scenarios with high mobility rates, the alignment timer could be much longer and coarse for alignment detection and establishment. Hence, the mutual alignment between two transceivers might not be preserved during a complete alignment period, a situation which needs to be carefully modeled in the simulation setup. Once the alignment timer expires, it takes one primary transceiver at a time and creates a list of candidate transceivers that both the primary transceiver and candidate transceiver are in each others’ line-of-sight, hence the term mutual alignment.

Figure 2 depicts the set of possible events that may occur before the alignment timer goes off in a scenario with multiple transceivers each from different nodes (A, B, C and D) with only their first transceiver shown and from A.1’s perspective. In the simplest case, alignments can stay unmodified like in Figure 2(a). In Figure 2(b), we see that node C moved and its transceiver C.1 can not see transceiver A.1 any more. But, transceiver A.1 can still see C.1 and because the alignment timer has not fired yet, A.1 continues to keep an entry for C.1 in its alignment list thinking that it is still aligned. Notice that, if the alignment timer expires in such a case, C.1 will not be placed in A.1’s list since the alignment between the two is lost and not *mutual*. That is, in our simulations the alignment is “bi-directional” and both A.1 and C.1 should see each other in order for communication to take place. Note that this is a conservative assumption for line-of-sight establishment and there is still room for improvement.

For the third case in Figure 2, C.1 might have turned its back or just moved out of line-of-sight of A.1. Hence both have lost alignment with each other and although they will continue to keep entries for each other packets will be dropped until the alignment timer expires and the alignments are re-established through other transceivers or paths.

The fourth case in Figure 2 is a new transceiver, D.1, gets in the LOS of A.1. However, D.1 and A.1 will not be able to exchange data packets until the alignment timer goes off again and the alignment lists are updated. This is another major conservative assumption in our simulations and is true; regardless of the alignment’s nature, uni-directional or bi-directional. If D.1 keeps staying in LOS of A.1, new entries will be created for each other in their alignment lists when the alignment timer expires. Only after then, the two transceivers will be able to exchange packets.

4. RESULTS

To show that our FSO simulation modules comply with the theoretical propagation model, we have done several simulation experiments. Our experiments involved two transceivers positioned in different ways with respect to each other. We observed received power and error probability while varying important parameters like the separation between the two transceivers, visibility and noise.

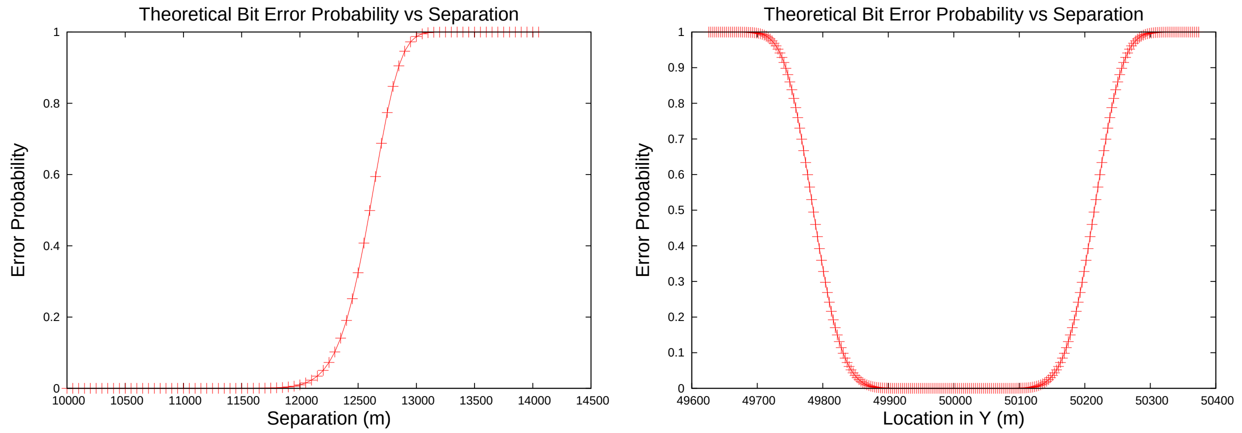

(a) Theoretical bit error probability increases as the receiver is moved away from the transmitter.

(b) Theoretical bit error probability increases as the receiver is moved away from the normal of the transmitter. Samples are taken with 2000 m separation from transmitter.

Figure 6. Theoretical error probability versus separation in both X and Y axis.

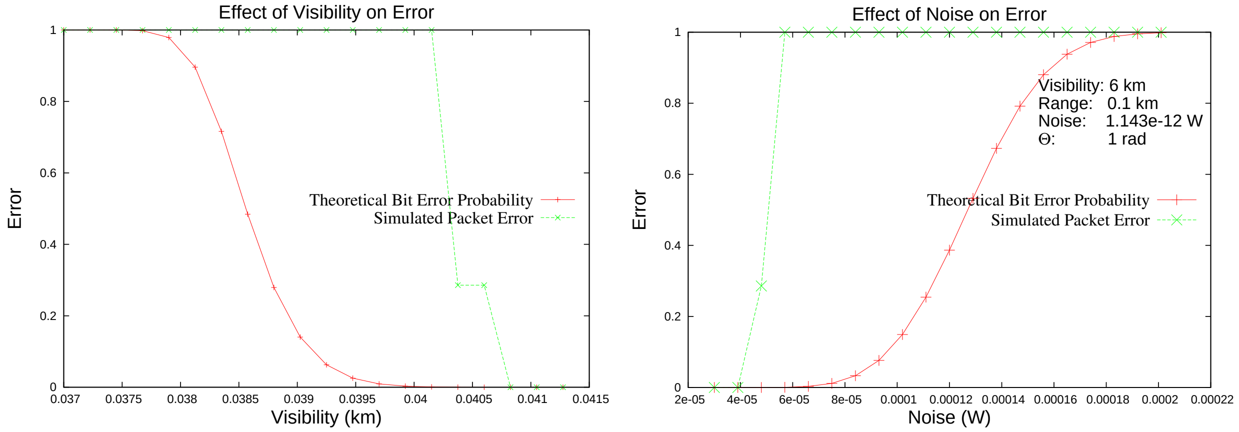

(a) Probability of error decreases as the visibility in the medium is increased. Percentage of delivered packets follows a similar but coarser grained behavior.

(b) Theoretical error probability and simulated packet error increase as the noise is increased.

Figure 7. Change in theoretical error probability with respect to visibility and noise.

4.1 Effect of Separation in Received Power and Theoretical Bit Error Probability

Complying with theoretical framework, our results reveal that the received power follows Lambertian law[11] from the transmitter itself and normal of the transmitter as depicted in Figure 5(a) and 5(b). Original transmission power for this scenario is calculated for 10 meter. We increased separation between transmitter and receiver antennas from 0.01 meter to 50 meters in our simulations. Figure 5(b) shows the Gaussian distribution of the received light intensity clearly as the receiver is moved away from transmitter's normal line at 5^{th} meter.

Distance also affects theoretical error probability since the received power decreases significantly. We sampled theoretical error with separation between antennas ranging from 10 km to 14 km. Figure 6(a) shows that the theoretical error probability increases significantly as the receiver is moved away from the transmitter while keeping the transmission power same following the power pattern shown in 5(a). Similarly, depicted error probability in Figure 6(b) increases as well as the receiver is mode away from the normal of the transmitter where the samples are taken at 2 km, since the received power decreases significantly (Figure 5(b).

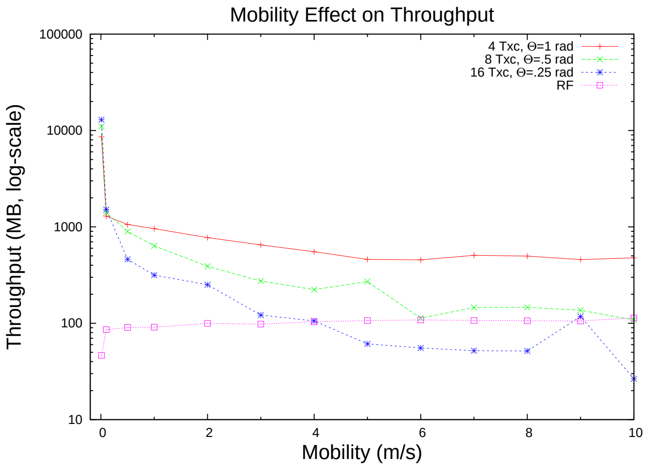

Figure 8. Effect of mobility of nodes on the overall network throughput.

4.2 Effect of Visibility in Theoretical Bit Error Probability and Simulated Packet Error

Low visibility in the medium makes the light experience more deviation from its intended direction by hitting aerosols in the air. This causes the received light intensity to drop which causes more bit errors. Hence, increasing visibility decreases theoretical error probability and simulated packet error. For this simulation scenario, the power is calculated for 100 meters with 6 km visibility and kept the same for all the simulations. Separation between antennas is 100 meters. We increased visibility from 0.037 km to 0.041275 km. In Figure 7(a), we show that the visibility in the medium affects theoretical bit error probability and simulated packet error significantly. From the figure, we can see that if visibility is set to a value from 0 to 0.037 km, the system experiences a high level of error and after 0.04 km, it recovers.

4.3 Effect of Background Noise in Theoretical Bit Error Probability and Simulated Packet Error

We found that noise has an important impact on theoretical bit error probability and simulated packet error since it will become harder for the receiver to operate at a low signal-to-noise ratio. We used a transmission power that reaches 100 meters with a noise level of 1.1428e-12 Watt for all of our simulations in this scenario. We increased the noise in the medium from 3.0e-5 W to 2.01e-4 W and found that both the theoretical error probability and simulated packet error are increased considerably as depicted in Figure 7(b).

4.4 Mobility Effect on Network Throughput

Our contribution to NS-2 enabled us to simulate FSO-MANETs and make accurate assessments. Our most important observation is that the mobility is the most fundamental factor that determines the end-to-end throughput. Figure 8 shows the effect of relative mobility of nodes on the network throughput where the mobility scenarios are generated using the random waypoint algorithm. Our conclusion is; increased mobility affects TCP adversely because of *intermittent connectivity* of nodes, especially when the nodes accommodate a large number of transceivers with small divergence angles. To compare with RF, FSO performs much better while the mobility is low and starts to get affected as we increase the speed of the nodes while still delivering better results if the divergence angle is large.

5. SUMMARY

In this paper, we presented our contribution to NS-2 in simulating free-space-optical communication links. While implementing NS-2 modules for FSO communications, we took visibility in the medium, divergence angles of transmitters, field of view of photo-detectors, and surface areas of transceiver devices into account. We validated the results of our modules against the well-known theoretical models on FSO propagation. Specifically, we compared the theoretical error probability and simulated packet error with respect to key FSO parameters such as separation, medium visibility and noise. We also looked at the drop in received power against these FSO parameters.

As another key dimension, we modeled multiple transceivers in our NS-2 modules for FSO. Our modules can simulate FSO structures with many transceivers placed at various shapes such as sphere or array. Further, our modules can simulate mobile scenarios for such multi-transceiver FSO structures. We believe that our simulation modules can help filling the urgent need for understanding how viable and promising FSO is as a general-purpose communication medium for mobile and/or wireless networking.

ACKNOWLEDGMENTS

This work is supported in part by NSF awards 0721452 and 0721612.

REFERENCES

[1] NRC Committee on Broadband Last Mile Technology, [*Broadband: Bringing Home the Bits*], National Research Council, CSTB (2002).

[2] Moral, A. R., Bonenfant, P., and Krishnaswamy, M., "The optical internet: architectures and protocols for the global infrastructure of tomorrow," *IEEE Communications Magazine* **39**(7), 152–159 (2001).

[3] Hunter, D. K. and Andonovic, I., "Approaches to optical internet packet switching," *IEEE Communications Magazine* **38**(9), 116–122 (2000).

[4] Ozgur, A., Levesque, O., and Tse, D., "Hierarchical cooperation achieves optimal capacity scaling in ad hoc networks," *IEEE Transactions on Information Theory* **53**, 3549–3572 (February 2007).

[5] Lomba, C. R., Valadas, R. T., and de Oliveira Duarte, A. M., "Efficient simulation of the impulse response of the indoor wireless optical channel," *Proc. of the Seventh IEEE International Symposium on Personal, Indoor and Mobile Communications* , 257–261 (1996).

[6] Joseph, J. B., Barry, J. R., Kahn, J. M., Krause, W. J., Lee, E. A., and Messerschmitt, D. G., "Simulation of multipath impulse response for indoor wireless optical channels," *IEEE Journal on Selected Areas in Comm* **11**, 367–379 (1993).

[7] Safari, M. and Uysal, M., "Relay-assisted free-space optical communication," *Signals, Systems and Computers, 2007. ACSSC 2007. Conference Record of the Forty-First Asilomar Conference on* , 1891 –1895 (Nov. 2007).

[8] Navidpour, S., Uysal, M., and Kavehrad, M., "BER performance of free-space optical transmission with spatial diversity," *Wireless Communications, IEEE Transactions on* **6**, 2813 –2819 (August 2007).

[9] Valadas, R., "Interference modelling for the simulation of ieee 802.11 infrared local area networks," *Personal, Indoor and Mobile Radio Communications, 1996. PIMRC'96., Seventh IEEE International Symposium on* **1**, 257 –261 vol.1 (Oct 1996).

[10] "The Network Simulator." `http://www.isi.edu/nsnam/ns/`.

[11] Willebrand, H., [*Free Space Optics*], Sams Pubs (2001). 1st Edition.

[12] Van de Hulst, H. C., [*Light Scattering by Small Particles*], John Wiley and Sons (1957).

[13] Perkins, C., "Ad hoc on demand distance vector (aodv) routing." IETF, Internet Draft, draft-ietf-manet-aodv-00.txt, November 1997 (1997).

[14] Yuksel, M., Akella, J., Kalyanaraman, S., and Dutta, P., "Free-space-optical mobile ad hoc networks: Auto-configurable building blocks," *ACM Springer Wireless Networks* **15**, 295–312 (April 2009).

[15] Bilgi, M. and Yuksel, M., "Multi-element free-space-optical spherical structures with intermittent connectivity patterns," in [*Proceedings of IEEE INFOCOM Student Workshop*], (2008).

[16] Nakhkoob, B., Bilgi, M., Yuksel, M., and Hella, M., "Multi-transceiver optical wireless spherical structures for manets," *IEEE Journal on Selected Areas of Communications* **27**(9) (2009).